

RSC Advances



This is an *Accepted Manuscript*, which has been through the Royal Society of Chemistry peer review process and has been accepted for publication.

Accepted Manuscripts are published online shortly after acceptance, before technical editing, formatting and proof reading. Using this free service, authors can make their results available to the community, in citable form, before we publish the edited article. This *Accepted Manuscript* will be replaced by the edited, formatted and paginated article as soon as this is available.

You can find more information about *Accepted Manuscripts* in the [Information for Authors](#).

Please note that technical editing may introduce minor changes to the text and/or graphics, which may alter content. The journal's standard [Terms & Conditions](#) and the [Ethical guidelines](#) still apply. In no event shall the Royal Society of Chemistry be held responsible for any errors or omissions in this *Accepted Manuscript* or any consequences arising from the use of any information it contains.

1 ***Hardening process and properties of an epoxy resin with bio-based***
2 ***hardener derived from furfural***

3
4 *Yuya Tachibana,^{a,b} Junko Torii,^a Ken-ichi Kasuya,^{a*} Masahiro Funabashi^c and Masao Kunioka^c*

5 ^aDivision of Chemistry and Chemical Biology, Graduate School of Science and Engineering, Gunma University, 1-5-1
6 Tenjin, Kiryu, Gunma 376-8515, Japan. E-mail: kkasuya@gunma-u.ac.jp

7 ^bJapan Science and Technology Agency (JST), 1-5-1 Tenjin, Kiryu, Gunma 376-8515, Japan.

8 ^cNational Institute of Advanced Industrial Science and Technology (AIST), Higashi 1-1-1, Tsukuba, Ibaraki 305-8565,
9 Japan.

10
11 ***Abstract***

12 The development of bio-based plastics is an important research area because of its contribution to
13 environmental preservation. Herein, we evaluated the properties of a bio-based epoxy resin synthesised using
14 2,2-bis(4-glycidyloxyphenyl)propane as the epoxy monomer and oxabicyclodicarboxylic anhydride (OBCA)
15 as a bio-based hardener derived from furfural. The major hardening process of the resin at 130°C, manifested
16 in an exponential increase in the storage modulus, was complete within an hour, which was longer than that
17 for a commercially available petroleum-based epoxy resin hardened using *cis*-cyclohexane dicarboxylic
18 anhydride (CDCA). This indicated that OBCA was less reactive than CDCA, which has a similar structure.
19 The bio-based epoxy resin showed excellent transparency in the visible light region and was thermally stable,
20 with 5% weight loss at temperatures exceeding 270°C. Glass transition temperatures were above 100°C, and
21 mechanical properties were moderately better than those of the commercially available epoxy resin.
22 Moreover, the bio-based carbon content ranged from 21% to 53%, depending on the amount of OBCA added.
23 Thus, the bio-based OBCA is a good hardener for a bio-based epoxy resin that can be used as a value-added
24 material in industrial applications.

25

26 *Introduction*

27 The use of biomass resources contributes to the prevention of global warming and depletion of petroleum
28 resources. To reduce the amount of petroleum used for plastics production, the development of various
29 bio-based commodity plastics is an industrially and academically important area of research. The
30 biodegradable polymers poly(lactic acid) (PLA),^{1,2} produced from corn seed, and poly(hydroxy alkanate)
31 (PHA),³ produced from plant oil and sugar, were developed as commercially available bio-based materials.
32 Since this century, bio-based polyethylene⁴ produced from bio-ethanol and partially bio-based polyethylene
33 terephthalate,⁵ in which the ethylene glycol unit is produced from bio-ethanol, have been used in
34 manufacturing. The development of other commodity plastics such as polypropylene,⁶ polyvinyl chloride,⁶
35 and poly(butylene succinate)⁷ is also in progress.

36 Epoxy resin is one of the most important thermosetting resins for industrial applications such as
37 coating material for automobiles, ships, and bridges to prevent corrosion, sealant for electrical devices for
38 protection from air and moisture, and adhesive for buildings, automobiles, aircrafts, and sporting goods.^{8,9}
39 Epoxy resins comprise monomers that contain at least two epoxide groups and can react with polyfunctional
40 hardeners like amines, acid, alcohols, thiols, and anhydrides to give high-performance cross-linked resins. A
41 mixture of an epoxy monomer and hardener is usually cured by external stimulation such as UV irradiation
42 or heating to give epoxy resin, and the properties of the cured resin can be controlled by the hardener and
43 cure time. Compared to other commercially available polymers, some epoxy resins are expensive. However,
44 these are widely used in manufacturing because of their high performance and availability, which give added
45 value to the cost of material. Although the additional cost of production usually precludes the utilization of
46 bio-based epoxy resins in manufacturing, this can be outweighed by superior properties of these resins.

47 A few bio-based epoxy resins have been synthesised from bio-based epoxy monomers and
48 bio-based hardeners.^{10,11} Epichlorohydrin, which is generally used as an epoxy monomer, was synthesised

49 from glycerol derived from natural fat, which is a by-product of bio-diesel and a surfactant.¹² The hydroxyl
50 groups of lignin derivatives react with epichlorohydrin to give epoxy monomers.¹³ Recently, the conversion
51 and curing of itaconic acid was reported.¹⁴ Vegetable oil containing an unsaturated fatty acid moiety was also
52 converted to an epoxy monomer through epoxidation of the double bond.¹⁵ Bio-based polyfunctional
53 compounds like vegetable oil,¹⁶ polysaccharide,¹⁷ and polylysine¹⁸ were converted to hardeners with thiol or
54 amino groups. Cyclic acid anhydrides are usually used as a hardener in manufacturing, and bio-based acid
55 anhydrides can be obtained from abietic acid or maleopimarate.¹⁹

56 The bio-based carbon content, defined as the ratio of carbons derived from biomass to the total
57 carbon of the material, has been established in ASTM, CEN, and ISO,²⁰ and is thus an objective standard to
58 evaluate bio-based materials. The amount of hardener in an epoxy resin is substantial, usually over 30%.
59 Therefore, the bio-based carbon content of an epoxy resin is sufficient for a bio-based polymer, even if only
60 the hardener is derived from biomass.

61 We have focused on furan derivatives produced from cellulose and hemicellulose as biomass
62 resources to produce polymers. Furan derivatives, such as 5-hydroxymethylfurfural (HMF), furfural, furfuryl
63 alcohol, and furan, are produced from biomass resources and used industrially as organic solvents or
64 resins.²¹⁻²⁴ The U.S. Department of Energy has stated that these are the most value-added chemicals derived
65 from biomass.²⁵ Therefore, considerable effort has been expended in their efficient conversion from biomass
66 resources.²⁶⁻²⁸

67 Furfural was previously converted to oxabicyclodicarboxylic anhydride (OBCA) through the
68 synthetic route shown in Scheme 1. OBCA is known as norcantharidin, which is an anti-cancer drug.²⁹ Its
69 polymerization with diols leads to formation of bio-based polyoxabicyclates (POBCs) that can replace
70 commercially available transparent elastic polymers.³⁰ The properties of POBCs depend on the rigidity,
71 bulkiness, and reactivity of OBCA, which is an oxo-bridged cyclohexane dicarboxylic anhydride.

72

73 [Scheme 1]

74

75 In this study, we demonstrate that OBCA can act as a bio-based hardener using
76 2,2-bis(4-glycidyloxyphenyl)propane (BADGE) as the epoxy monomer and tetraphenylphosphonium
77 bromide (TPPB) as the catalyst to obtain a bio-based epoxy resin. BADGE has two epoxide groups and is
78 formed by the condensation between bisphenol A and epichlorohydrin. It is a commercially available epoxy
79 monomer widely used in manufacturing.³¹ To evaluate OBCA as a hardener, a commodity epoxy resin was
80 also synthesised for comparison using *cis*-cyclohexane dicarboxylic anhydride (CDCA). The hardening
81 process of each epoxy resin was evaluated as time-dependent properties using dynamic mechanical analysis
82 (DMA) at the hardening temperature. The chemical structure after hardening was analysed using Fourier
83 transform infrared (FT-IR) spectroscopy. Optical properties were evaluated using ultraviolet-visible (UV-vis)
84 spectroscopy. Thermal stability was measured using thermal gravimetric analysis (TGA). The mechanical
85 properties of the moulded specimens were assessed based on tensile strength and temperature-dependent
86 DMA. The latter was also used to obtain thermal properties.

87

88 **Experimental**

89 **Materials**

90 2,2-Bis(4-glycidyloxyphenyl)propane (BADGE), tetraphenylphosphonium bromide (TPPB), and
91 *cis*-cyclohexane dicarboxylic anhydride (CDCA) were purchased from Tokyo Kasei Industry Co., Ltd.
92 (Tokyo, Japan) and used without further purification. The synthesis of OBCA from furfural was described in
93 our previous study.³¹

94 Instrumentation

95 Pre-treatment was performed using a thermo-mighty stirrer (HHE-19G-USII; Koike Precision Instruments,
96 Hyogo, Japan) with an aluminium block bath. Compressed moulding was done using a hot-pressing machine
97 (Mini Press Test 10; Toyo Seiki Seisaku-sho Ltd., Tokyo, Japan). FT-IR spectra were obtained using an
98 FT-IR spectrophotometer (Nicolet iS50 FT-IR; Thermo Fisher Scientific K.K., Yokohama, Japan) equipped
99 with a single-reflection attenuated total reflectance (ATR) system (Spectra-Tech Foundation Performer).
100 Thermal stability was determined by thermal gravimetric analysis (TGA-50; Shimadzu Co., Kyoto, Japan)
101 conducted up to 500°C at a rate of 10°C/min. The transparency of 0.10-mm-thick epoxy resin films was
102 measured using a UV-vis spectrophotometer (UV-1700; Shimadzu Co., Kyoto, Japan) in the wavelength
103 range 190–1100 nm. Dynamic mechanical properties were measured using a dynamic mechanical analyser
104 (DMA8000; PerkinElmer Inc., Waltham, MA, USA) in single cantilever bending mode at an oscillatory
105 frequency of 1.0 Hz and an applied deformation of 0.05 mm during heating. To measure the thermal
106 properties, *i.e.*, storage modulus (E') and $\tan \delta$ (E''/E'), as a function of temperature, temperature scans from
107 0°C were performed at a heating rate of 2°C/min. The kinetics was measured isothermally at 130°C, and E'
108 and $\tan \delta$ were recorded as a function of time (min). The strength and strain of the specimens at breaking
109 point were measured at room temperature by performing tensile strength tests with a universal material
110 testing machine (EZ-test; Shimadzu). The grip distance was 10 mm and the speed rate of the tensile strength
111 test was 10 mm/min.

112 General procedure for time-dependent DMA

113 BADGE (449 mg, 1.32 mmol) and dicarboxylic anhydride (2.10 mmol) were added to a 2-ml disposable test
114 tube. After stirring the mixture vigorously at 100°C for 10 min to dissolve the acid anhydride, TPPB (4 mg,
115 10 μ mol) was added. The mixture was stirred with a magnetic stirrer at 100°C for 10 min. The resulting
116 viscous liquid (~5 mg) was placed on the Material Pocket and dynamic mechanical properties were measured.

117 The thermal program consisted of heating from 30 to 130°C at 20°C/min for 5 min and maintaining the
118 temperature at 130°C for 240 min.

119

120 [Fig. 1]

121

122 **General procedure for pressing moulding**^{31, 32}

123 The viscous liquid, as prepared above, was centrifuged to remove air bubbles. The transparent liquid was
124 then placed on a mould made of polypropylene (40 × 40 × 0.2 mm) and pressed at 5 MPa and 130°C for an
125 arbitrary amount of time.

126 **General procedure for tensile strength testing**

127 The compressed film was cut into specimens (20 mm long, 1.0 mm wide, 0.2 mm deep). The tensile strength
128 was taken as the maximum strength required to break the material on the stress-strain curve. The tensile
129 strain at the breaking point was taken as the maximum strain on the stress-strain curve. An average value for
130 each specimen was taken from several sample measurements under the same conditions.

131

132 [Scheme 2]

133

134 ***Results and Discussion***

135 **Hardening Process**

136 Thermal hardening with bio-based OBCA gave the bio-based epoxy resin **1** as shown in Scheme 2. To
137 evaluate the effect of the oxabicyclic moiety of OBCA on resin properties, CDCA was also used as a

138 hardener to give the commercially available epoxy resin **2**. CDCA has a similar structure to OBCA except for
139 the oxo bridge.

140 The thermal hardening process was investigated by carrying out a time-dependent dynamic
141 mechanical analysis based on isothermal measurements at ambient temperature. The rheology of the
142 hardening process is commonly evaluated by separately analysing the viscous liquid and solid material using
143 a rheometer and by dynamic mechanical analysis, respectively. However, it is possible to evaluate both states
144 using the latter with a Material Pocket made of stainless plate as done in this study. The pre-mixing viscous
145 liquid sample was placed between the two halves of the Material Pocket and compressed carefully to avoid
146 leakage as shown in Fig. 1. The sample was immediately heated to the hardening temperature within 5 min
147 and the temperature was kept constant while measuring isothermal properties. The changes in E' and $\tan \delta$
148 (Fig. 2) showed the hardening behaviour of **1** and **2** at different hardening temperatures.

149

150 [Fig. 2]

151

152 The value of E' at the initial temperature (0°C) was different from that at the hardening
153 temperature; however, this did not arise from the temperature difference, but from the use of the Material
154 Pocket to handle the sample in the DMA apparatus. The decrease in E' of **1** during heating to the isothermal
155 temperature indicates that the viscosity of the reaction mixture decreased with temperature. E' exponentially
156 increased after hardening to form the cross-linked network began (major hardening process), and almost
157 reached a plateau when hardening was nearly complete. The major hardening process at 110, 130, 150, and
158 179°C was almost done within 155, 43, 21, and 19 min, respectively; thus, as the hardening temperature
159 increased, the corresponding time shortened. On the other hand, the E' of **1** continued to increase gradually at

160 all temperatures even after the initial exponential rise and the elapsed time was over 250 min, which
161 indicates that a minor hardening process occurred even after the major one. This result coincided with those
162 of thermal gravimetric analysis and tensile strength testing as will be discussed below.

163 The time-dependent hardening behaviour of **2** at 130°C is shown in Fig. 3. The E' of **2**
164 exponentially increased between 5 and 16 min and then almost reached a plateau, similar to **1** (Fig. 2b),
165 although the increase for the latter occurred between 21 and 43 min. This indicated that the hardening
166 process of **2** at 130°C also began immediately and was nearly complete in 16 min. However, a minor
167 hardening process gradually continued after the major one. The change in the E' of **1** in this plateau region
168 was larger than that of **2**. This suggests that the reactivity of OBCA with BADGE was lower than that of
169 CDCA. The difference in reactivity can be attributed to the bulky oxabicyclic moiety of OBCA that sterically
170 hinders the acid anhydride moiety.

171

172 [Fig. 3]

173

174 In addition, the hardening behaviour of **1** and **2** indicates that the cross-linked network possibly
175 formed during the major hardening process while residual functional groups, such as epoxy and carboxylic
176 acid, possibly reacted in the cross-linked network during the minor hardening process. The change in
177 physical properties resulting from the minor hardening process was insignificant after 60 min at all
178 hardening temperatures; however, the change was smallest at 130°C. Hereafter, the properties of bio-based
179 epoxy resin **1** will be evaluated using the samples that hardened at 130°C.

180 The ratio between the epoxy and hardener usually affects the properties of the epoxy resin.⁸

181 Initially, an epoxy/hardener mole ratio of 1.32/2.10 was adopted. The E' and tan δ of **1** at a ratio of 1.32/0.94

182 and 1.32/3.96 are shown in Figs. 2e and 2f, respectively. The hardening time depended on the amount of
183 hardener. The major hardening process of **1** was complete at 22, 43, and 75 min using 0.94, 2.10, and 3.96
184 mmol of OBCA, respectively. As the amount of OBCA increased, the time required for the major hardening
185 process became longer. With a small amount of OBCA, the cross-linked network formed is low density.
186 Therefore, the hardening process could rapidly proceed because the hardener could easily move through the
187 low-density network. On the other hand, the hardening process became slower in proportion to the amount of
188 OBCA as the cross-linked network became denser. Furthermore, the high flexibility of the moulded film of **1**,
189 obtained using 0.94 mmol OBCA, compared with the other films indicates the formation of a low-density
190 cross-linked network. The physical properties of **1** obtained using 0.94 mmol OBCA are listed in Table 1.

191 The bio-based carbon contents of **1** and **2** are summarized in Table 1 as well. The bio-based
192 carbon contents of the epoxy resin hardened using 0.94, 2.10, and 3.96 mmol OBCA were 21, 38, and 53%,
193 respectively. This indicates that the bio-based carbon content of **1** can be easily increased by using the
194 bio-based hardener OBCA, which derives its carbons from bio-based furfural.

195

196 [Table 1]

197

198 **Chemical structure analysis**

199 The change in chemical structure after the hardening process was determined from the FT-IR spectra. The
200 peaks at 1607 and 1509 cm^{-1} observed in the BADGE spectrum shown in Fig. 4a were assigned to aromatic
201 stretching vibrations. OBCA and CDCA had several peaks around 1700–1800 cm^{-1} due to the aliphatic cyclic
202 acid anhydride. The peaks at 1842 and 1774 cm^{-1} observed in the OBCA spectrum (Fig. 4b) and those at
203 1856 and 1786 cm^{-1} observed in the CDCA spectrum (Fig. 4c) were assigned to symmetric and asymmetric

204 carbonyl stretching vibrations, respectively. After hardening for 4 h, these peaks disappeared and a peak at
205 1745 cm^{-1} assigned to the carbonyl ester stretching vibration appeared in the spectra of both **1** and **2** as
206 shown in Figs. 4e and 4g, respectively. These indicate that acid anhydrides reacted with epoxy groups to
207 yield esters, which formed the cross-linked network in the epoxy resin. On the other hand, the relative
208 intensities of the peak at 1509 cm^{-1} due to BADGE and that at 1745 cm^{-1} due to the ester bond formed by
209 hardening changed with the amount of OBCA as shown in Figs. 4d-f.

210 When the amount of OBCA used in **1** was 3.96 mmol, the peak at 1856 cm^{-1} due to acid anhydride
211 was still observed 4 h from the beginning of hardening as shown in Fig. 4f. Although one BADGE molecule
212 having two epoxide groups can theoretically react with four OBCA molecules, it was difficult to complete
213 the hardening process with stoichiometric amounts of OBCA and BADGE owing to the high-density
214 cross-linked network, which could interfere with the reaction between the epoxide and acid anhydride. If the
215 reaction proceeds stoichiometrically, the epoxy resin becomes a fragile material owing to the presence of
216 four OBCA units at the termini of bisphenol A. Therefore, residual OBCA was left from the initial 3.96
217 mmol after the four-hour hardening process.

218 As mentioned above, the hardening process did not reach completion after 4 h. We then attempted
219 to identify the residual functional groups during the hardening of **1** with 0.94 mmol OBCA. Each
220 sample of **1** and **2** was prepared as a 0.2-mm-thick film at different hardening times (1, 2, 3, and 4 h) by the
221 hot-pressing method at 5 MPa and 130°C . All epoxy resin films were transparent and hard at each hardening
222 time. However, the residual functional groups could not be identified as the difference in the hardening time
223 was not manifested in the IR spectra.

224

225 [Fig. 4]

226

227 **Thermal stability**

228 The dependence of thermal stability on the hardening time was evaluated using thermal
229 gravimetric analysis conducted up to 500°C under a nitrogen atmosphere. The TGA curves are shown in Fig.
230 5 and 5% weight loss temperatures ($T_{d5\%}$) are summarized in Table 1. No dependency of $T_{d5\%}$ on the
231 hardening time and amount of OBCA was observed. This result indicates that the thermal stability did not
232 depend on the minor hardening process. The $T_{d5\%}$ of **1** at different hardening times was comparable to that of
233 **2**, demonstrating that the oxabicyclic moiety in **1** hardly affected the thermal stability of the epoxy resin.
234 Thus, the thermal stability of **1** was as good as that of **2**, which is currently used in industries.

235

236 [Fig. 5]

237

238 **Optical property**

239 Optical properties were measured using UV-vis spectroscopy. No clear relationship between transparency
240 and hardening time was observed as in the thermal gravimetric analysis. Therefore, only the spectra of **1** and
241 **2** hardened for 4 h are shown in Fig. 6. The decrease in the transparency of **2** was initially gradual from 330
242 nm and became steeper from 300 nm. On the other hand, the transparency of **1** gradually decreased from 390
243 nm and then sharply decreased from 340 nm. Subsequently, specific absorption was observed around 310–
244 320 nm. Since this difference between the transparency of **1** and **2** was observed in all samples hardened for
245 1, 2, 3, and 4 h, it can be attributed to the difference in the chemical structure of the anhydride moiety of the
246 hardeners. The UV-vis spectra of the monomers are shown in Fig. 7. BADGE and TPPB had a strong
247 absorption band below 300 nm due to the aromatic ring. While CDCA had a strong absorption band below

248 280 nm due to the carbonyl double bond, no strong absorption band was observed for OBCA above 260 nm.
249 These indicate that the side reaction of OBCA reported previously³⁰ occurred during the hardening process
250 and some resulting functional groups had absorption between 310 and 350 nm. Although we attempted to
251 determine these functional groups using FT-IR analysis, the characteristic peaks were not observed.

252

253 [Fig. 6]

254 [Fig. 7]

255

256 **Dynamic mechanical properties**

257 To evaluate the thermal properties of **1** and **2** hardened at 130°C for 4 h, dynamic mechanical analysis was
258 performed with varying temperature, from 0°C at a heating rate of 2°C/min. The E' and tan δ of **1** using 0.92,
259 2.10, or 3.96 mmol OBCA and **2** are shown in Fig. 8. The glass transition temperature (T_g), the temperature
260 at which tan δ was a maximum, is summarized in Table 1. The E' of **1** using 0.94, 2.10, and 3.96 mmol
261 OBCA was 3.8, 3.4, and 3.3 GPa, respectively, at 25°C. These results indicate that there is no significant
262 relationship between E' and the amount of OBCA.

263 On the other hand, the T_g of **1** increased with increasing amount of OBCA. Thus, a large amount
264 of OBCA led to the formation of a high-density cross-linked network, resulting in a heat-resistant epoxy
265 resin. The T_g of **1** hardened using 0.94 mmol OBCA was around room temperature; therefore, this moulded
266 sample was more flexible than the others. In comparison, the E' and T_g of **2** using 2.10 mmol CDCA were 3.1
267 GPa and 93°C. T_g is an important parameter to consider in choosing an epoxy resin for industrial use. The T_g
268 of **1** was above the boiling point of water (100°C) while that of **2** was not, which makes the thermal
269 properties of the former superior to the latter.

270

271 [Fig. 8]

272

273 **Tensile strength**

274 The mechanical properties of **1** and **2** hardened at 130°C at 5 MPa were determined using tensile strength
275 testing. Young's modulus, tensile strength, and strain at breaking point are summarized in Table 1. The
276 tensile strength of **1** was almost the same as that of **2**, while strain at breaking point of **1** was smaller than
277 that of **2**. This suggests that the oxabicyclic moiety in **1** hindered the elongation owing to its bulkiness and
278 imparted hardness to the sample. With increasing hardening time, Young's modulus and the tensile strength
279 of **1** increased and those of **2** decreased, while the strain at breaking point of **1** decreased and that of **2**
280 increased. These results suggest that the hardening process of **1** and **2** gradually continued even after the
281 major hardening process was complete, as explained above.

282 The mechanical properties of **1** using 0.94 mmol OBCA indicate that it is more flexible than other
283 epoxy resins owing to its low-density cross-linked network. Conversely, **1** using 3.96 mmol OBCA was more
284 fragile than others owing to its high-density cross-linked network.

285

286 **Conclusion**

287 A novel bio-based epoxy resin was successfully synthesised using the bio-based acid anhydride OBCA
288 derived solely from furfural. The bio-based carbon content of the epoxy resins was 21–53 % depending on
289 the amount of OBCA added. Isothermal measurements using the dynamic mechanical analyser demonstrated
290 that the major hardening process was complete within 1 h. On the other hand, the rate of hardening with
291 OBCA was slower than with CDCA owing to the bulkiness and lower reactivity of the former. Nevertheless,

292 **1** was found to be thermally stable as an epoxy resin. Although the transparency of **1** was excellent in the
293 visible light region, the absorption band of a by-product derived from OBCA was observed below 380 nm.
294 The high T_g of **1** compared to **2** indicated that OBCA imparted thermal resistance to epoxy resins. Finally, its
295 mechanical properties were almost the same as those of **2**. These favourable features of **1** can be attributed to
296 the effect of the oxabicyclic moiety. In addition, the side reaction of this moiety, which was also observed in
297 our previous study on polyesters containing OBCA,³¹ enhanced the physical properties of the epoxy resin.
298 Thus, **1** is suitable for industrial applications and preferable to **2** because it is a bio-based material.

299 Although BADGE was chosen as the epoxy in this study to evaluate OBCA as a hardener, other
300 epoxies including the bio-based ones that were previously reported can also be used.¹⁰⁻¹³ A bio-based epoxy
301 and bio-based OBCA hardener will thus give a fully bio-based epoxy resin.

302

303 **Acknowledgment**

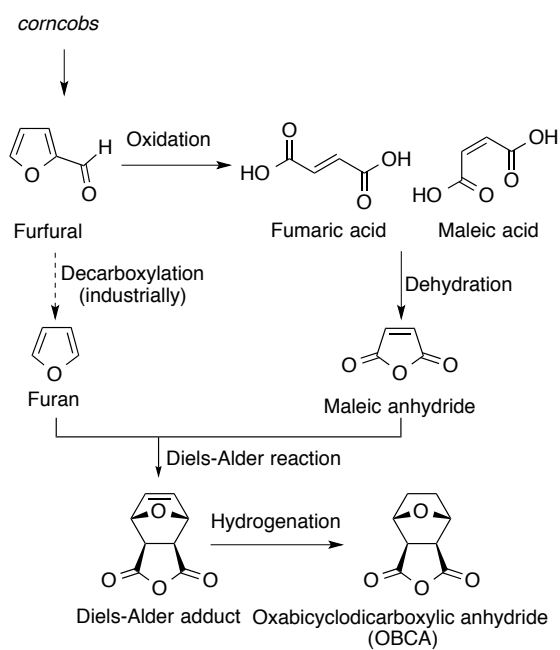
304 This work, under the project “Creation of essential technologies to utilize carbon dioxide as a resource
305 through the enhancement of plant productivity and the exploitation of plant products,” was supported by the
306 Precursory Research for Embryonic Science and Technology (PRESTO) program of the Japan Science and
307 Technology Agency (JST).

308

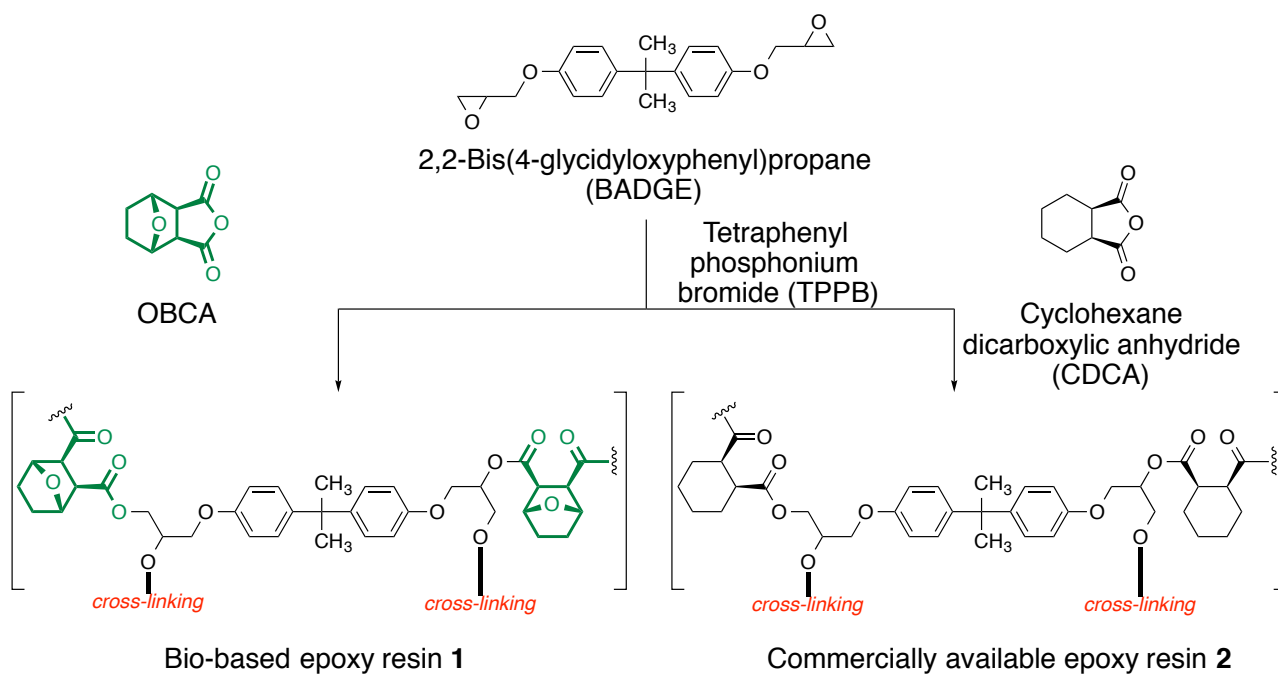
309 **References**

- 310 1. J. Lunt, *Polym. Degrad. Stab.*, 1998, **59**, 145.
311 2. E. T. H. Vink, K. R. Rábago, D. A. Glassner and P. R. Gruber, *Polym. Degrad. Stab.*, 2003, **80**, 403.
312 3. K. Sudesh, H. Abe and Y. Doi, *Prog. Polym. Sci.*, 2000, **25**, 1503.
313 4. A. Morschbacker, *Polym. Rev.*, 2009, **49**, 79.
314 5. R. Mülhaupt, *Macromol. Chem. Phys.*, 2013, **214**, 159.
315 6. R. T. Mathers, *J. Polym. Sci., Part A: Polym. Chem.*, 2012, **50**, 1.
316 7. Y. Tachibana, T. Masuda, M. Funabashi and M. Kunioka, *Biomacromolecules*, 2010, **11**, 2760.
317 8. *Epoxy Polymers: New Materials and Innovations*, ed. J.-P. Pascault and R. J. J. Williams, Wiley-VCH, Weinheim,
318 2010.
319 9. R. S. Bauer, in *Applied Polymer Science*, eds. R. W. Tess and G. W. Poehlein, American Chemical Society,
320 Washington, DC, 2nd edn., ACS Symposium Series 285, 1985, pp. 931–961.
321 10. R. Auvergne, S. Caillol, G. David, B. Boutevin and J.-P. Pascault, *Chem. Rev.*, 2014, **114**, 1082.
322 11. J.-M. Raquez, M. Deléglise, M.-F. Lacrampe and P. Krawczak, *Prog. Polym. Sci.*, 2010, **35**, 487.
323 12. L. Shen, E. Worrell and M. Patel, *Biofuels, Bioprod. Biorefin.*, 2010, **4**, 25.
324 13. T. Koike, *Polym. Eng. Sci.*, 2012, **52**, 701.

- 325 14. S. Ma, X. Liu, Y. Jiang, Z. Tang, C. Zhang and J. Zhu, *Green Chem.*, 2013, **15**, 245.
326 15. M. Galià, L. M. de Espinosa, J. C. Ronda, G. Lligadas and V. Cádiz, *Eur. J. Lipid Sci. Technol.*, 2010, **112**, 87.
327 16. T. Takahashi, K. Hirayama, N. Teramoto and M. Shibata, *J. Appl. Polym. Sci.*, 2008, **108**, 1596.
328 17. N. Illy, S. Benyahya, N. Durand, R. Auvergne, S. Caillol, G. David and B. Boutevin, *Polym. Int.*, 2014, **63**, 420.
329 18. Y. Takada, K. Shinbo, Y. Someya and M. Shibata, *J. Appl. Polym. Sci.*, 2009, **113**, 479.
330 19. H. Wang, X. Liu, B. Liu, J. Zhang and M. Xian, *Polym. Int.*, 2009, **58**, 1435.
331 20. M. Kunioka, K. Taguchi, F. Ninomiya, M. Nakajima, A. Saito and S. Araki, *Polymers (Basel)*, 2014, **6**, 423.
332 21. O. W. Cass, *Ind. Eng. Chem. Res.*, 1948, **40**, 216.
333 22. F. Trimble, *Ind. Eng. Chem.*, 1941, **33**, 660.
334 23. J. P. Trickey, C. S. Miner and H. J. Brownlee, *Ind. Eng. Chem.*, 1923, **15**, 65.
335 24. W. J. Mckillip, in *Adhesives from Renewable Resources*, eds. R. W. Hemingway, A. H. Conner and S. J. Branham,
336 American Chemical Society, Washington, DC, ACS Symposium Series 385, 1989, pp. 408–423.
337 25. J. J. Bozell and G. R. Petersen, *Green Chem.*, 2010, **12**, 539.
338 26. R. Weingarten, J. Cho, W. C. Conner, Jr. and G. W. Huber, *Green Chem.*, 2010, **12**, 1423.
339 27. P. L. Dhepe and R. Sahu, *Green Chem.*, 2010, **12**, 2153.
340 28. A. Cukalovic and C. V. Stevens, *Green Chem.*, 2010, **12**, 1201.
341 29. A. McCluskey and J. A. Sakoff, *Mini-Rev. Med. Chem.*, 2001, **1**, 43.
342 30. Y. Tachibana, M. Yamahata and K. Kasuya, *Green Chem.*, 2013, **15**, 1318.
343 31. *Japan Pat.*, A 2003-26763, 2003.
344 32. G. Pan, Z. Du, C. Zhang, C. Li, X. Yang and H. Li, *Polym. J.*, 2007, **39**, 478.



Scheme 1.



Scheme 2.

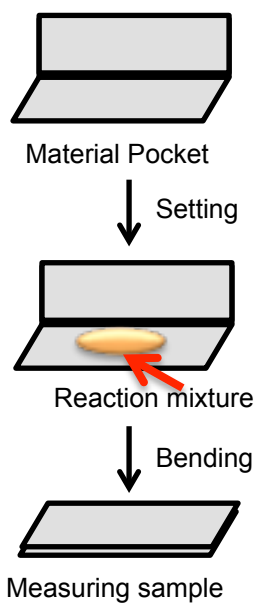
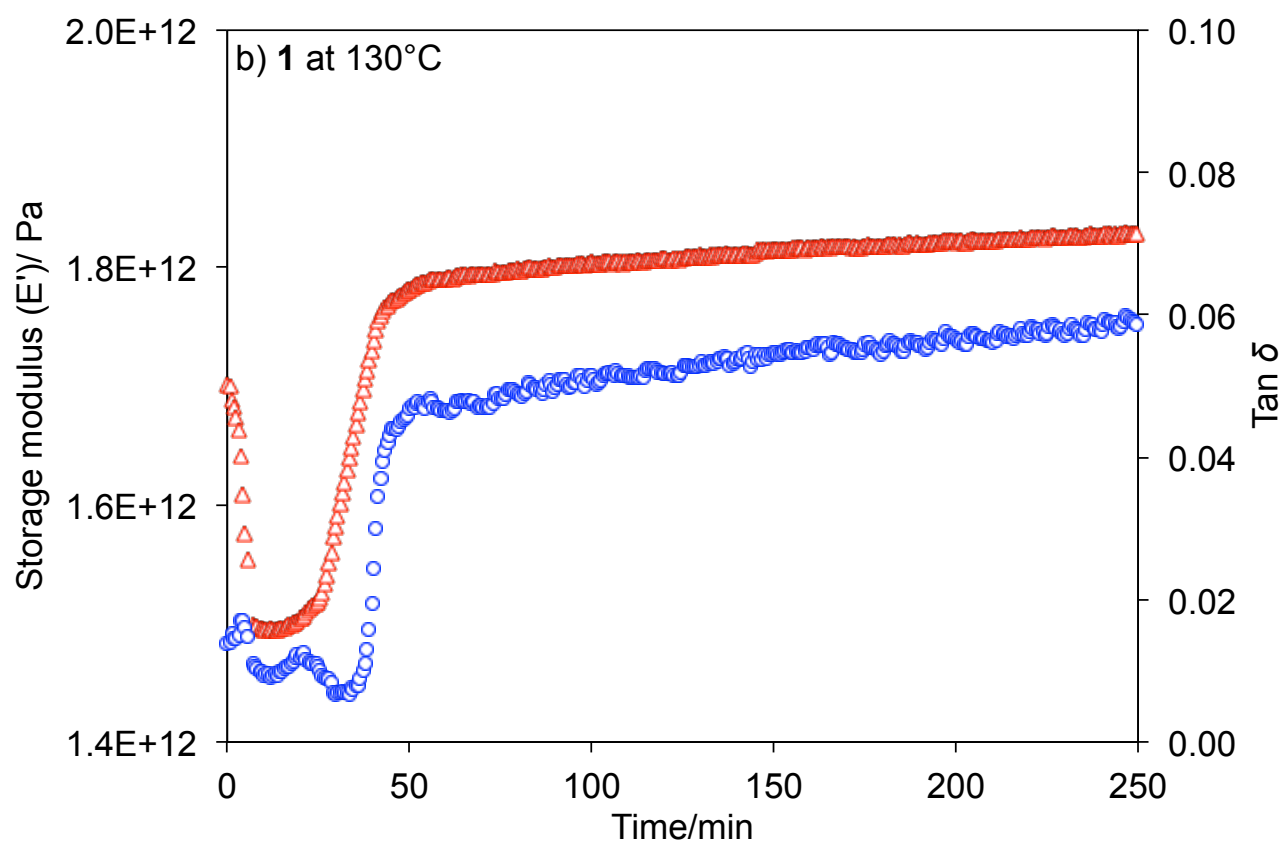
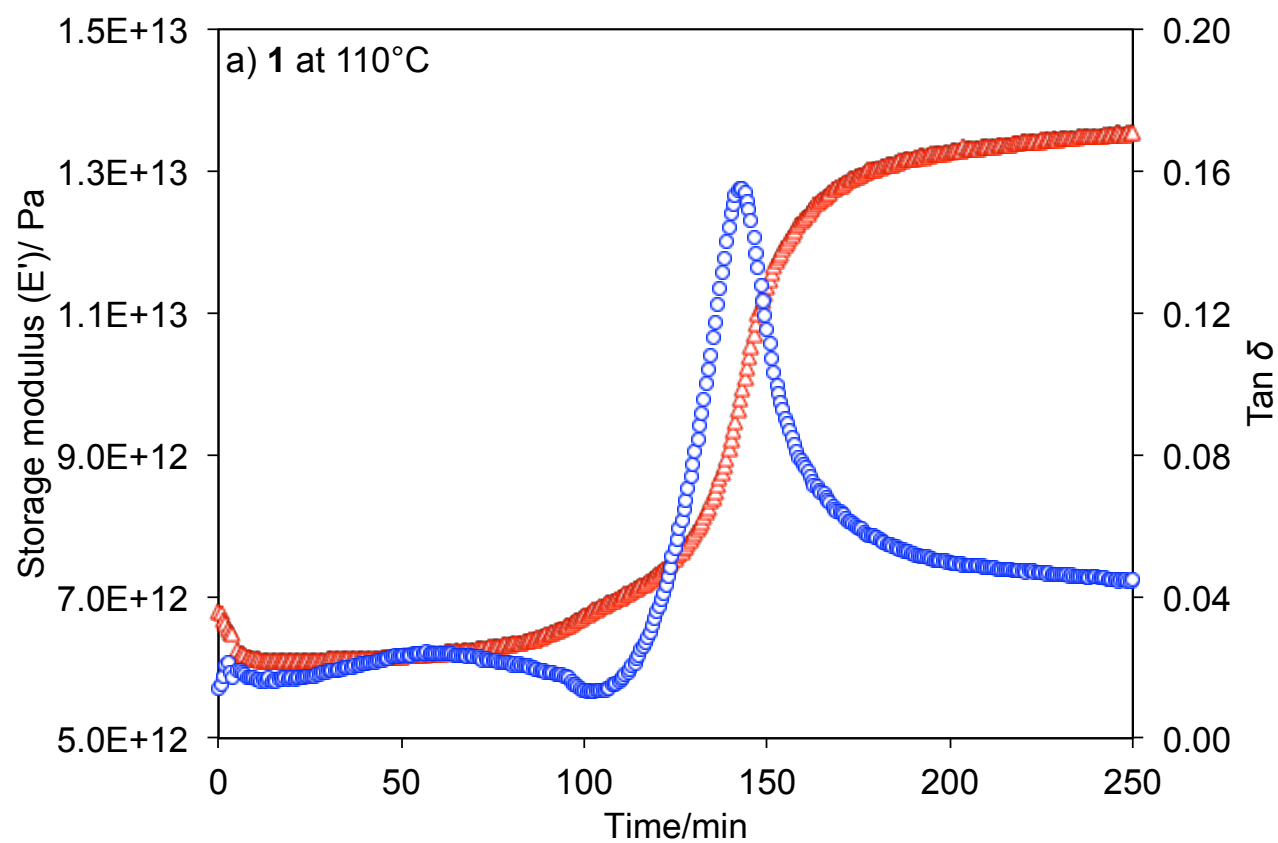
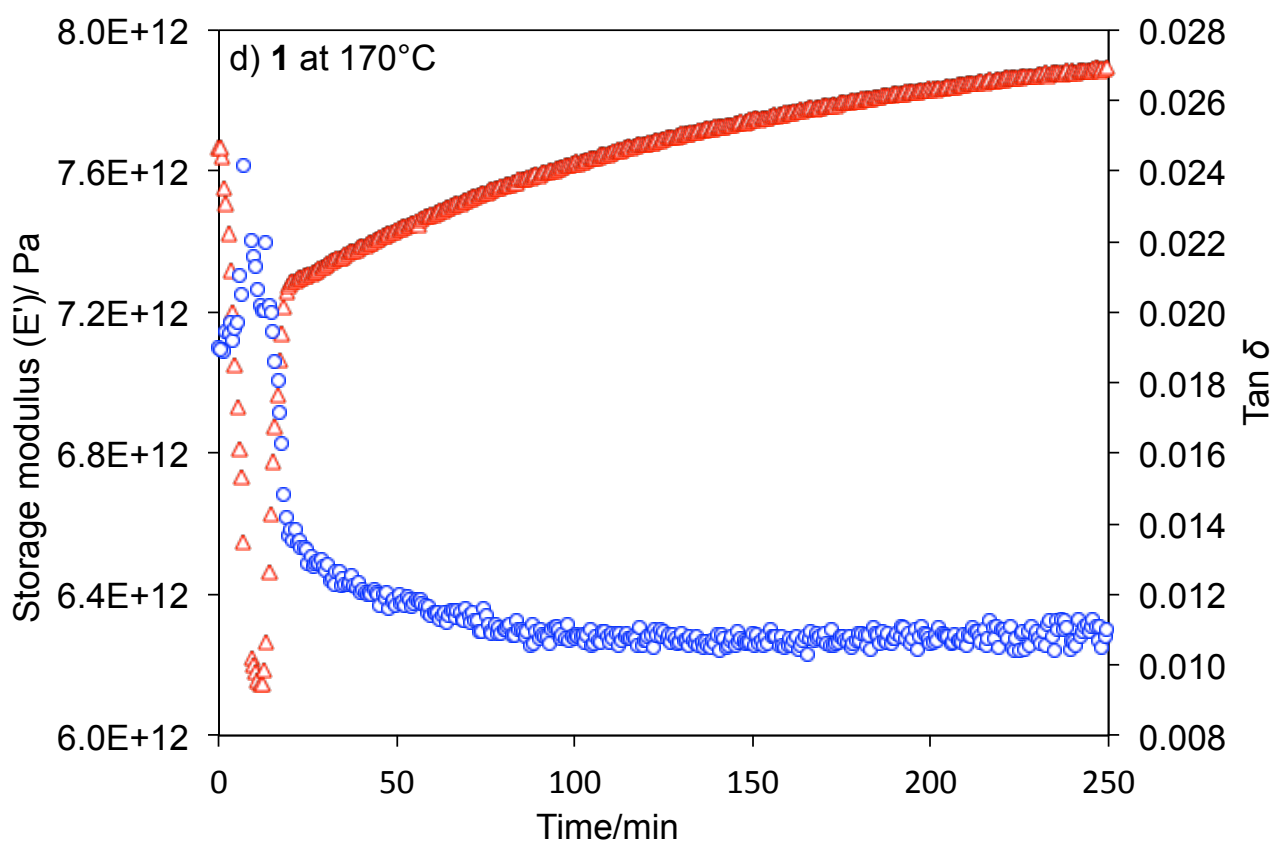
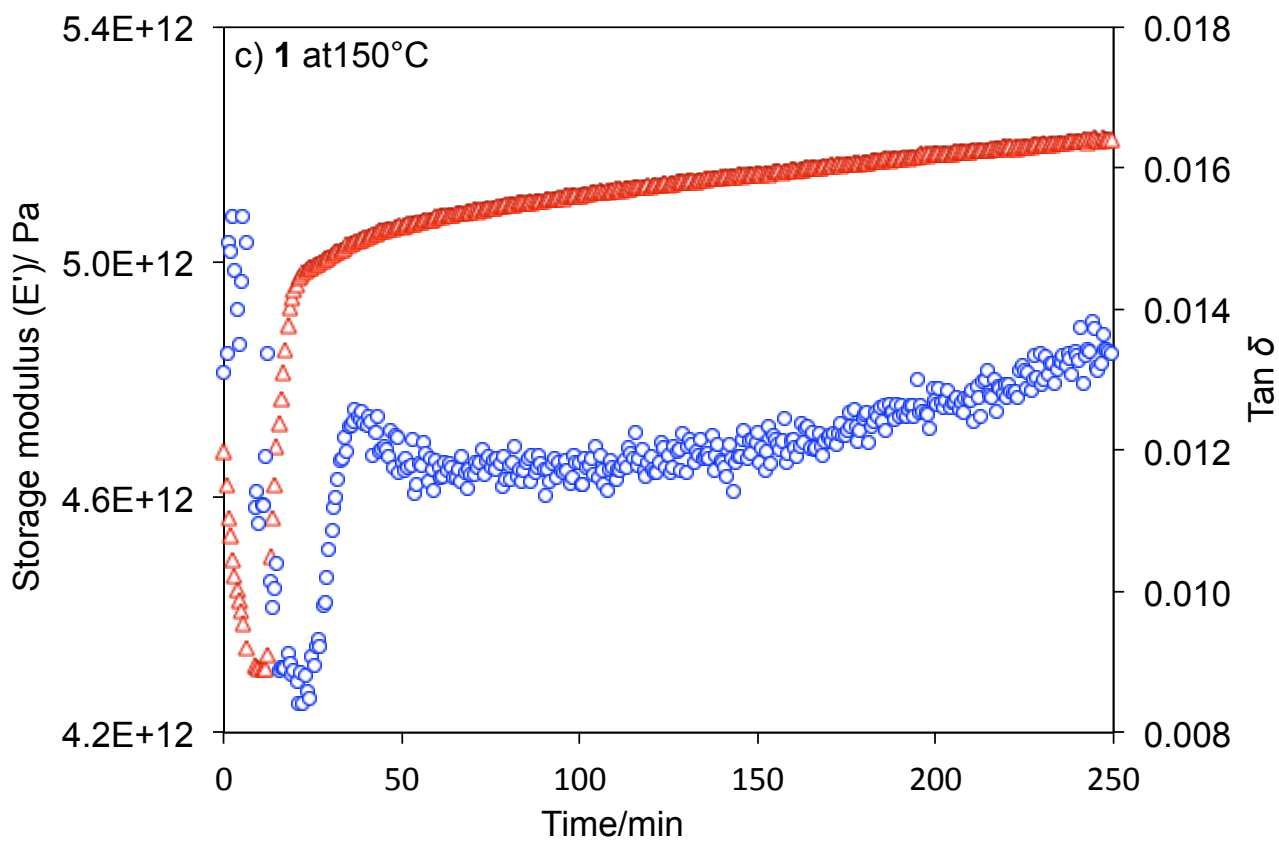


Fig. 1 Sample preparation method using Material Pocket.





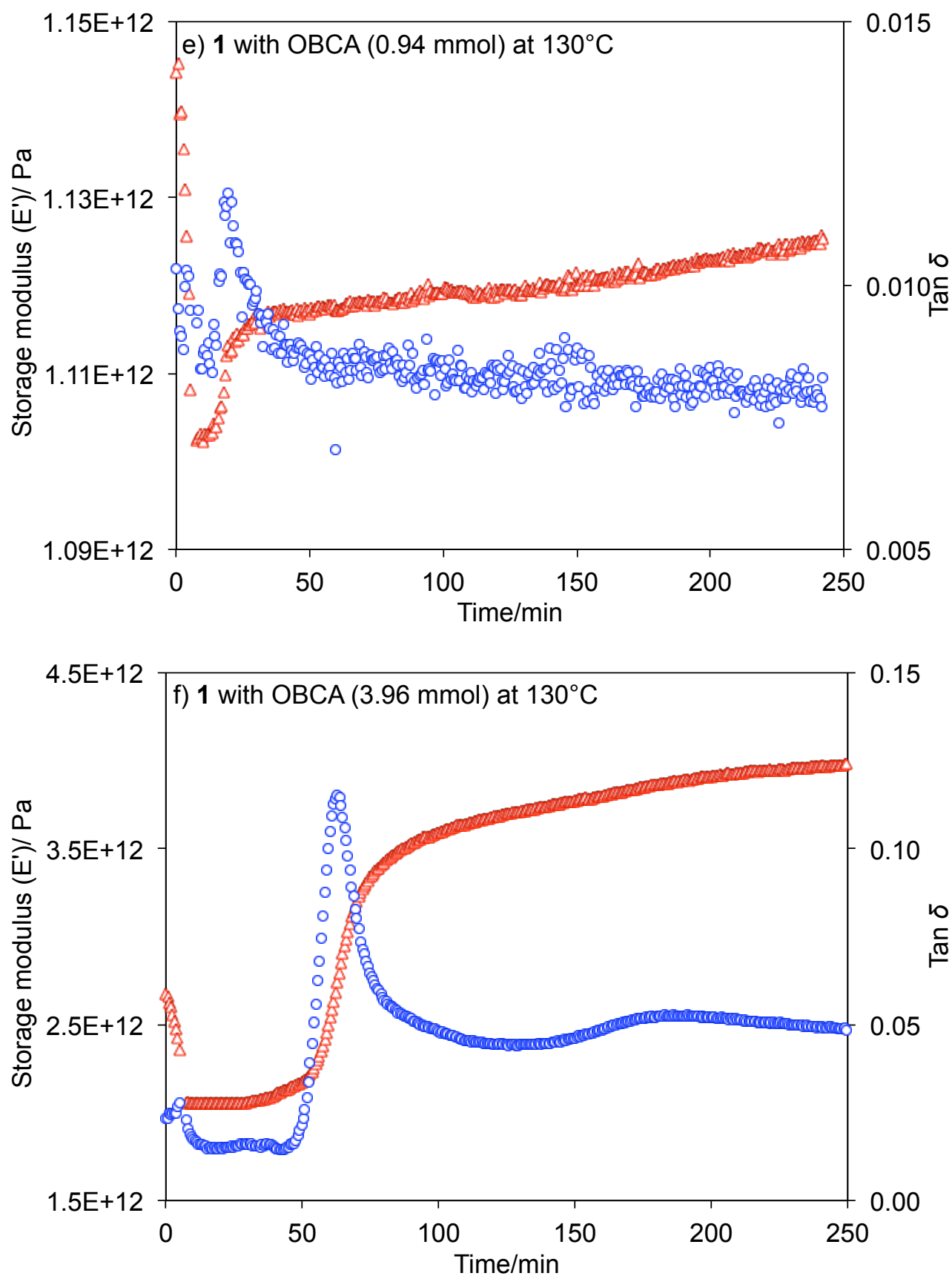


Fig. 2 Time-dependent dynamic mechanical analysis. Storage modulus E' (red open triangles) and $\tan \delta$ (blue open circles) of **1** at a) 110°C, b) 130°C, c) 150°C, d) 170 °C, e) 130°C with 0.94 mmol OBCA, and f) 130°C with 3.96 mmol OBCA during isothermal analysis.

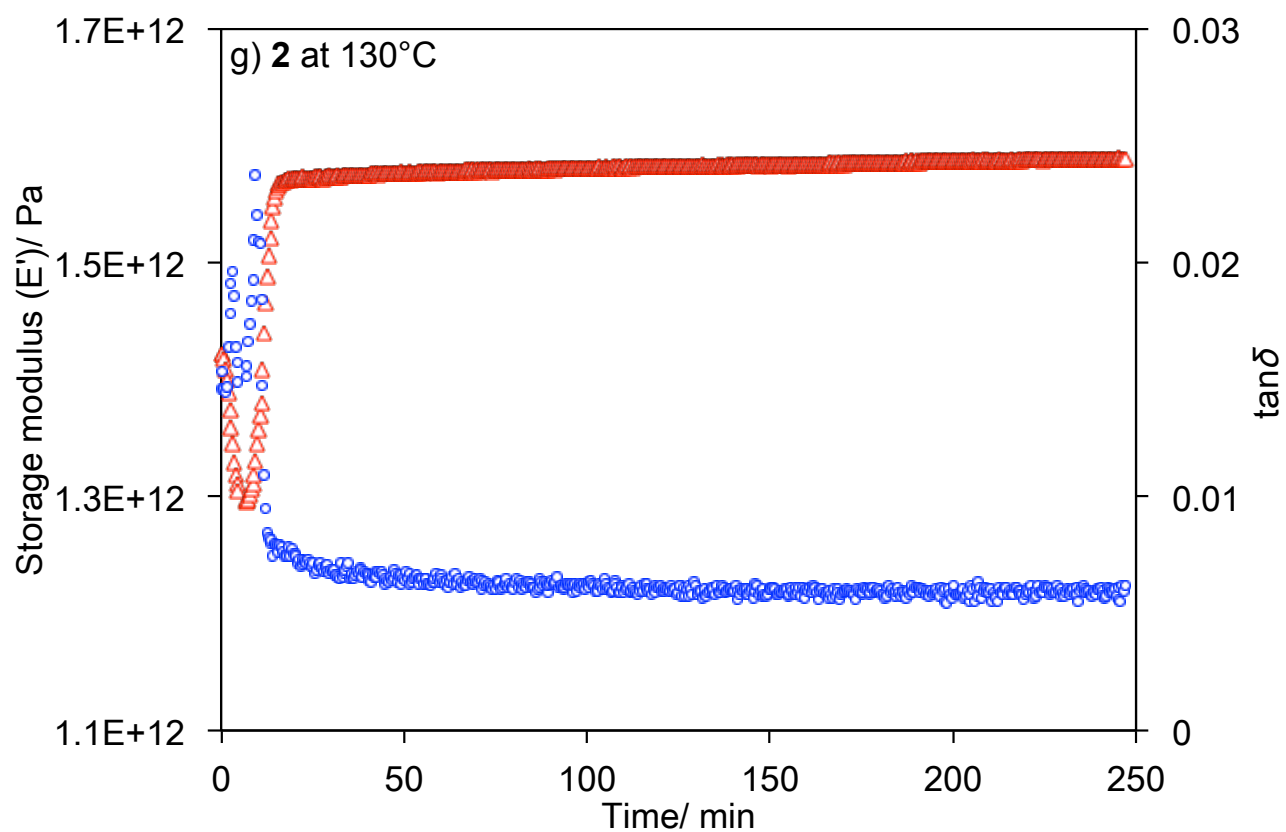


Fig. 3 Time-dependent dynamic mechanical analysis. Storage modulus E' (red open triangles) and $\tan \delta$ (blue open circles) of **2** at 130°C during isothermal analysis.

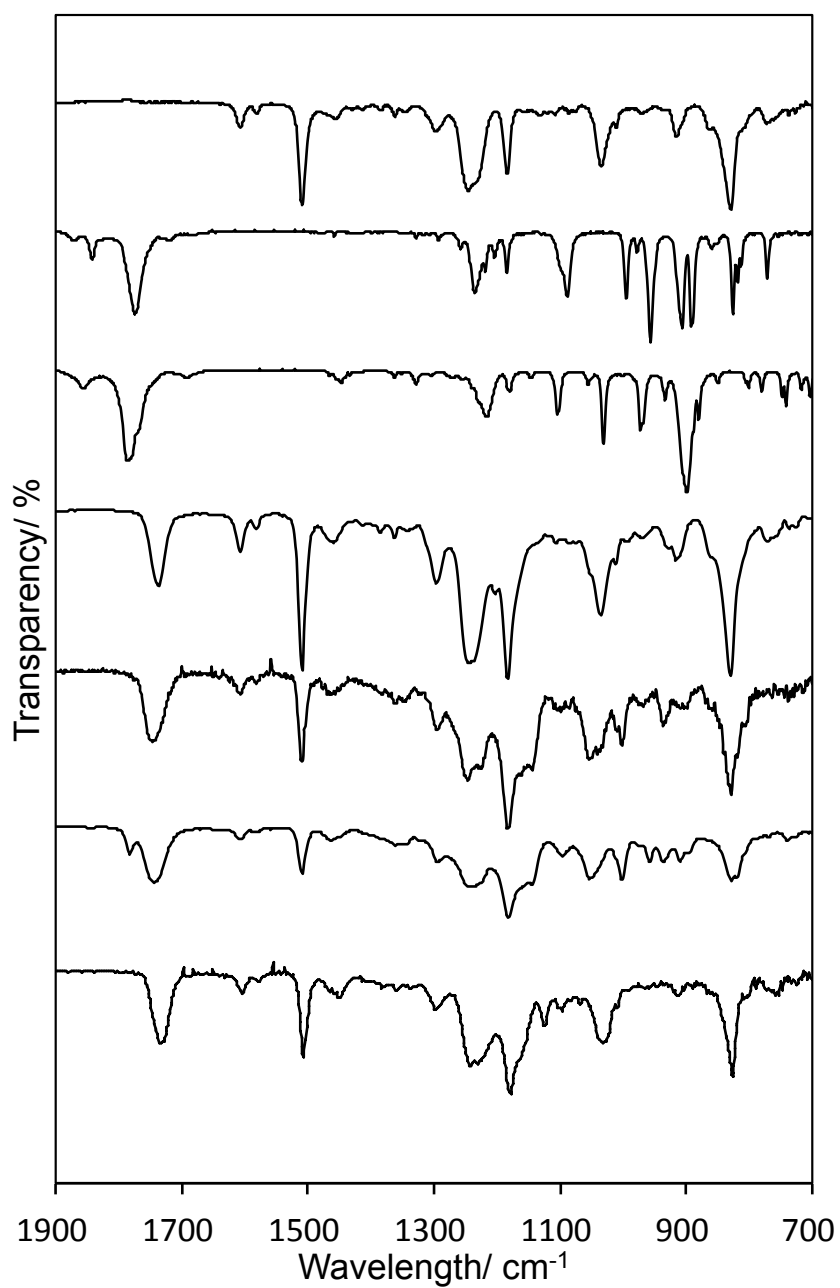


Fig. 4 IR spectra of a) BAGDE, b) OBCA, c) CDCA, d) **1** (0.94 mmol OBCA), e) **1** (2.10 mmol OBCA), f) **1** (3.96 mmol OBCA), and g) **2**.

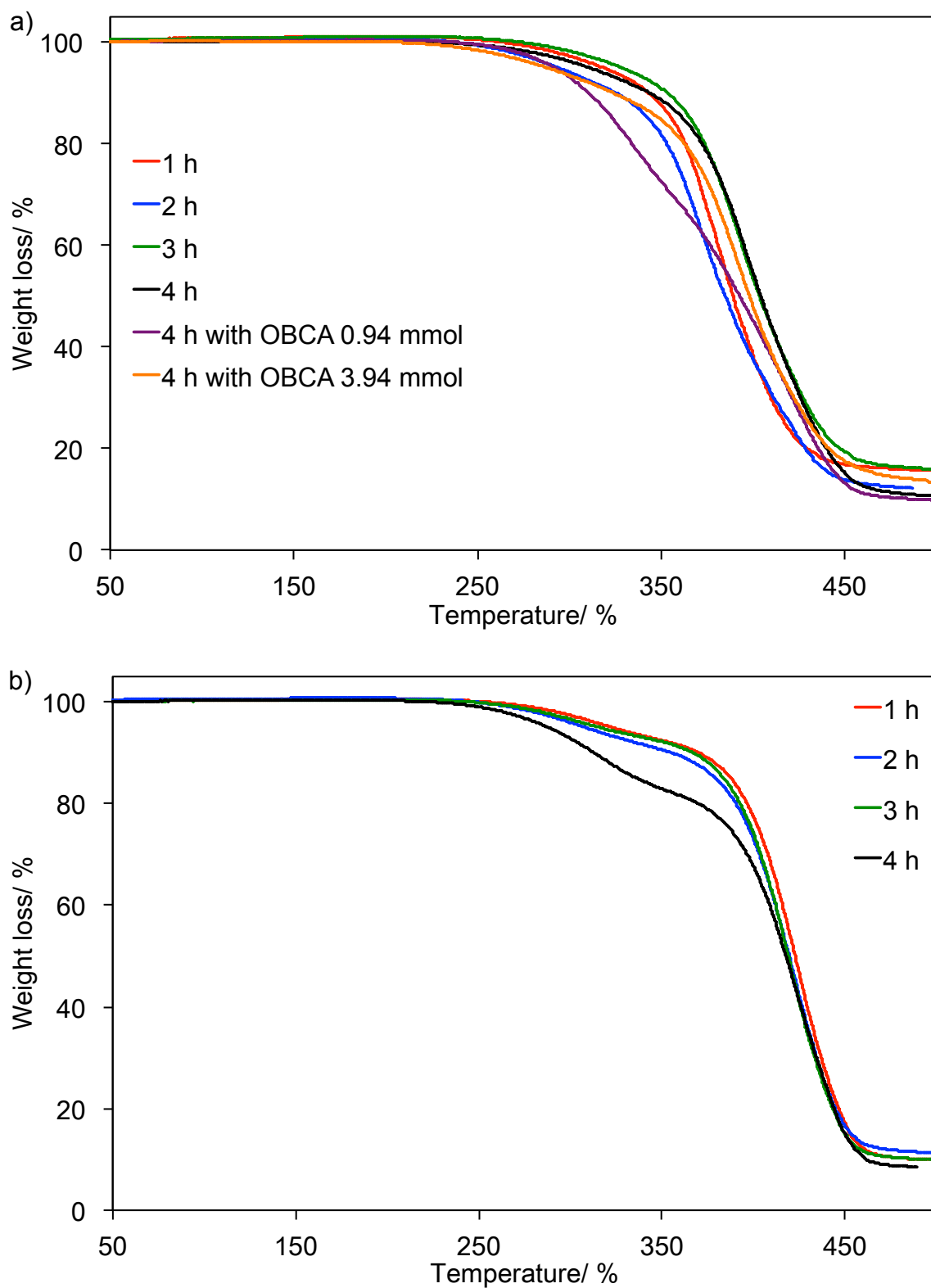


Fig. 5 Thermal gravimetric analysis curves of a) **1** and b) **2** at different hardening times.

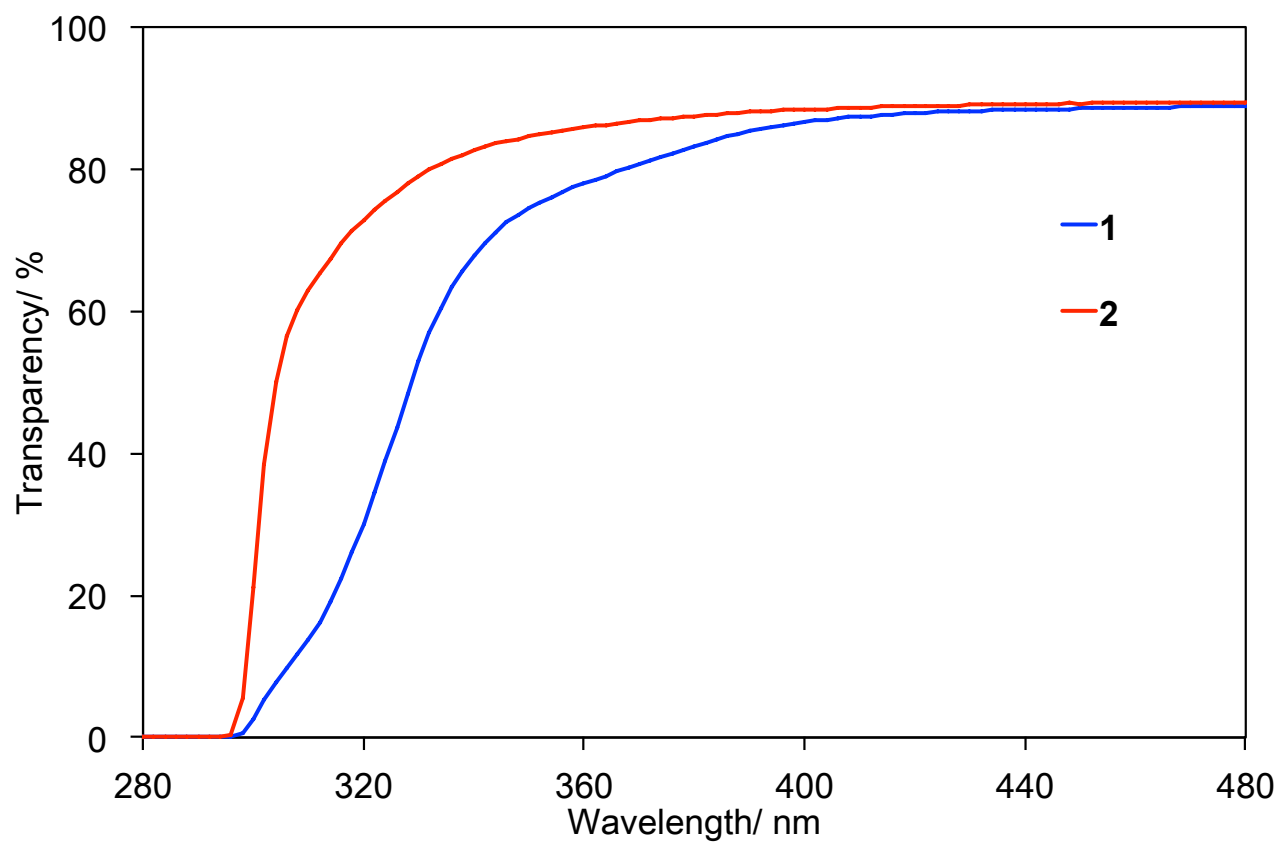


Fig. 6 Transparency of films of **1** and **2** hardened at 130°C for 4 h measured by UV-vis spectroscopy.

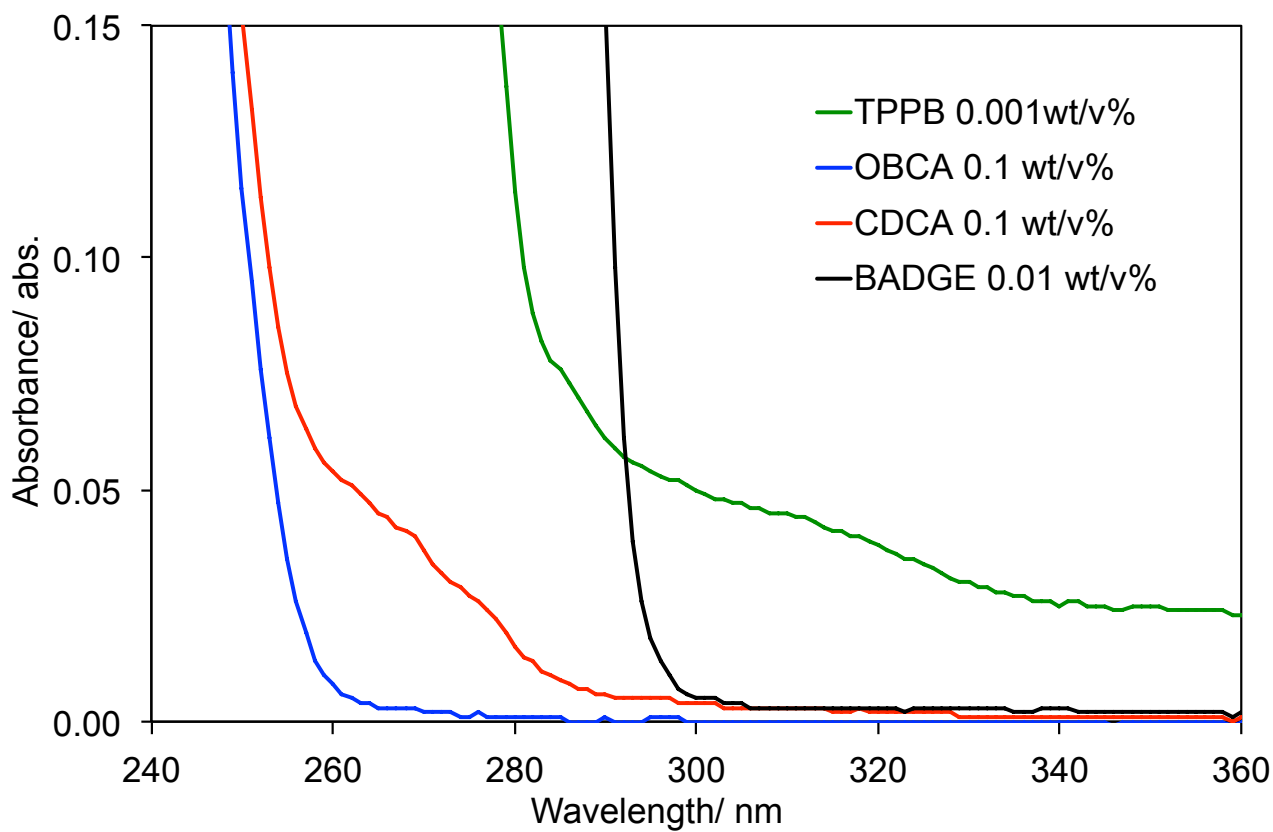
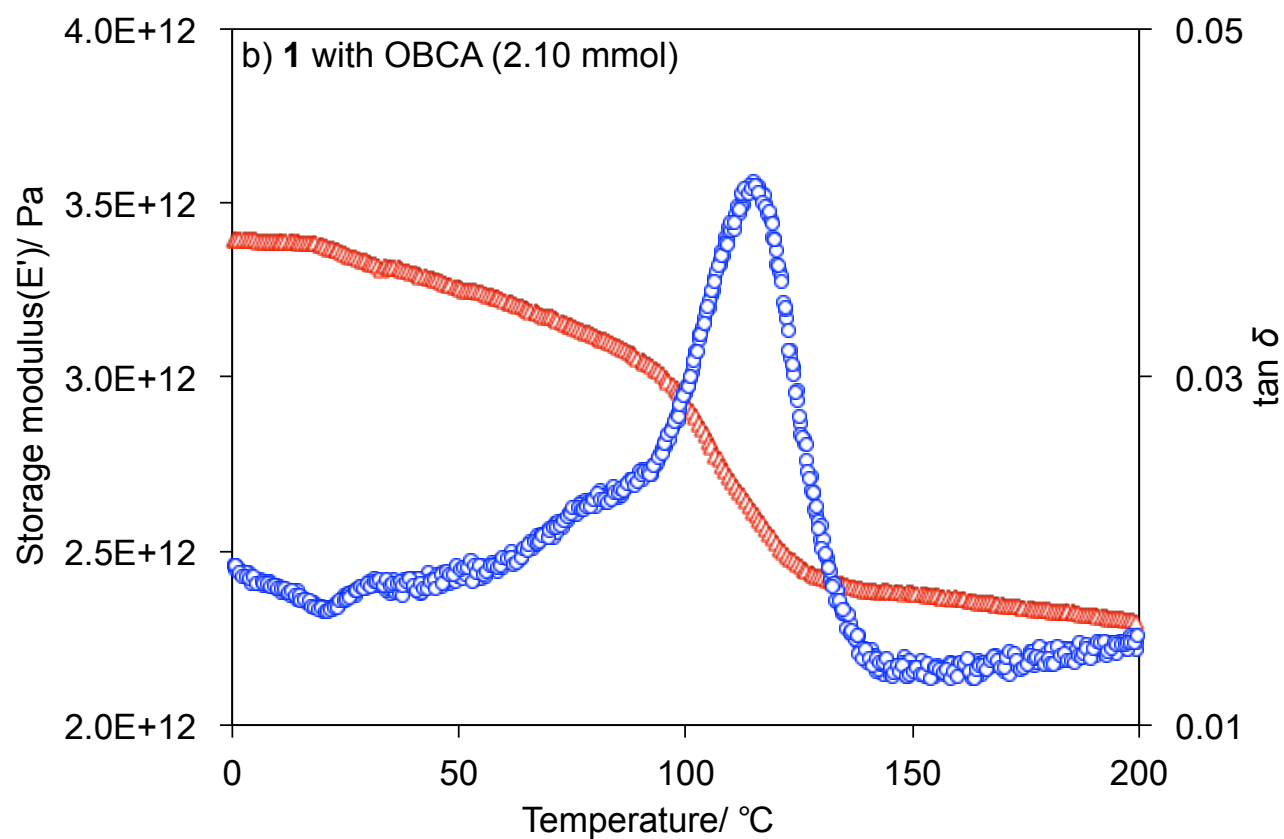
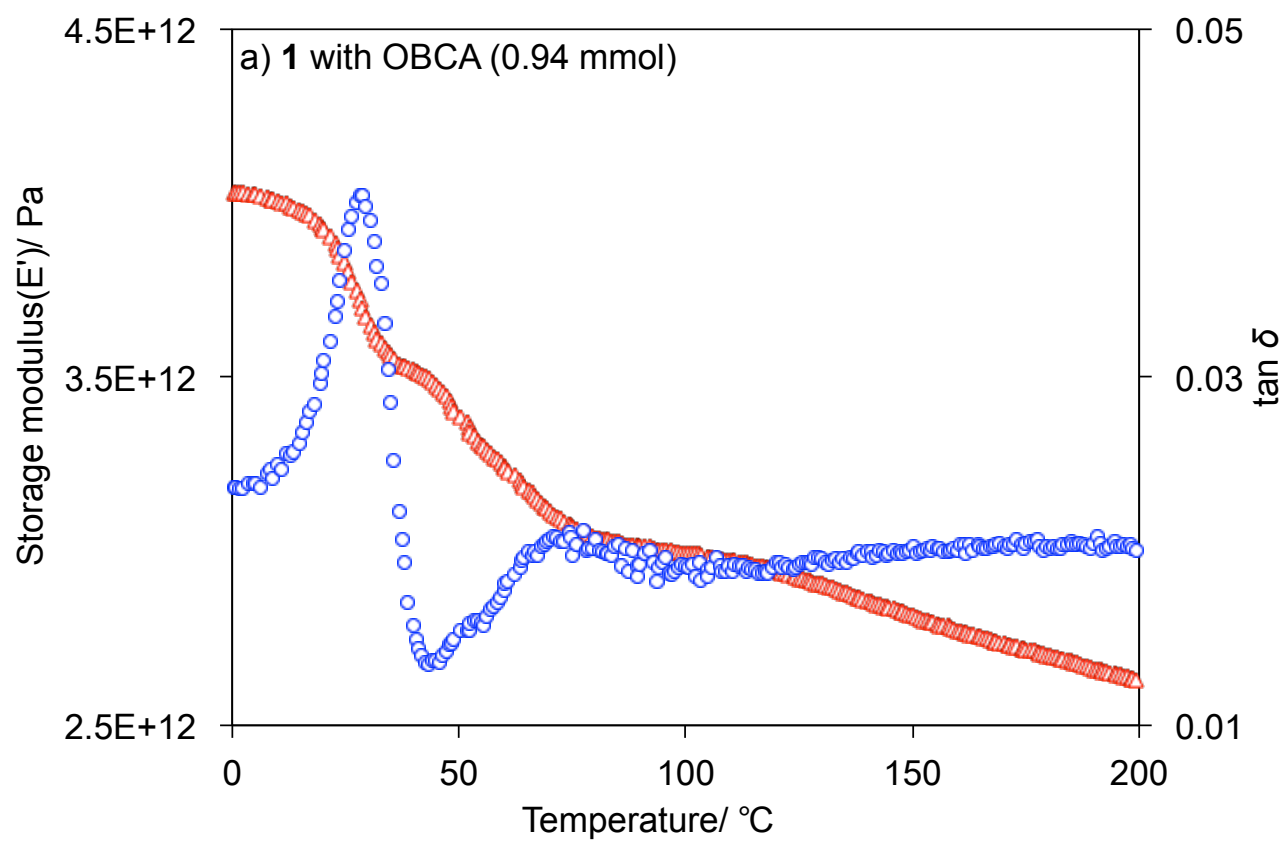


Fig. 7 UV-vis spectra of each monomer in acetonitrile.



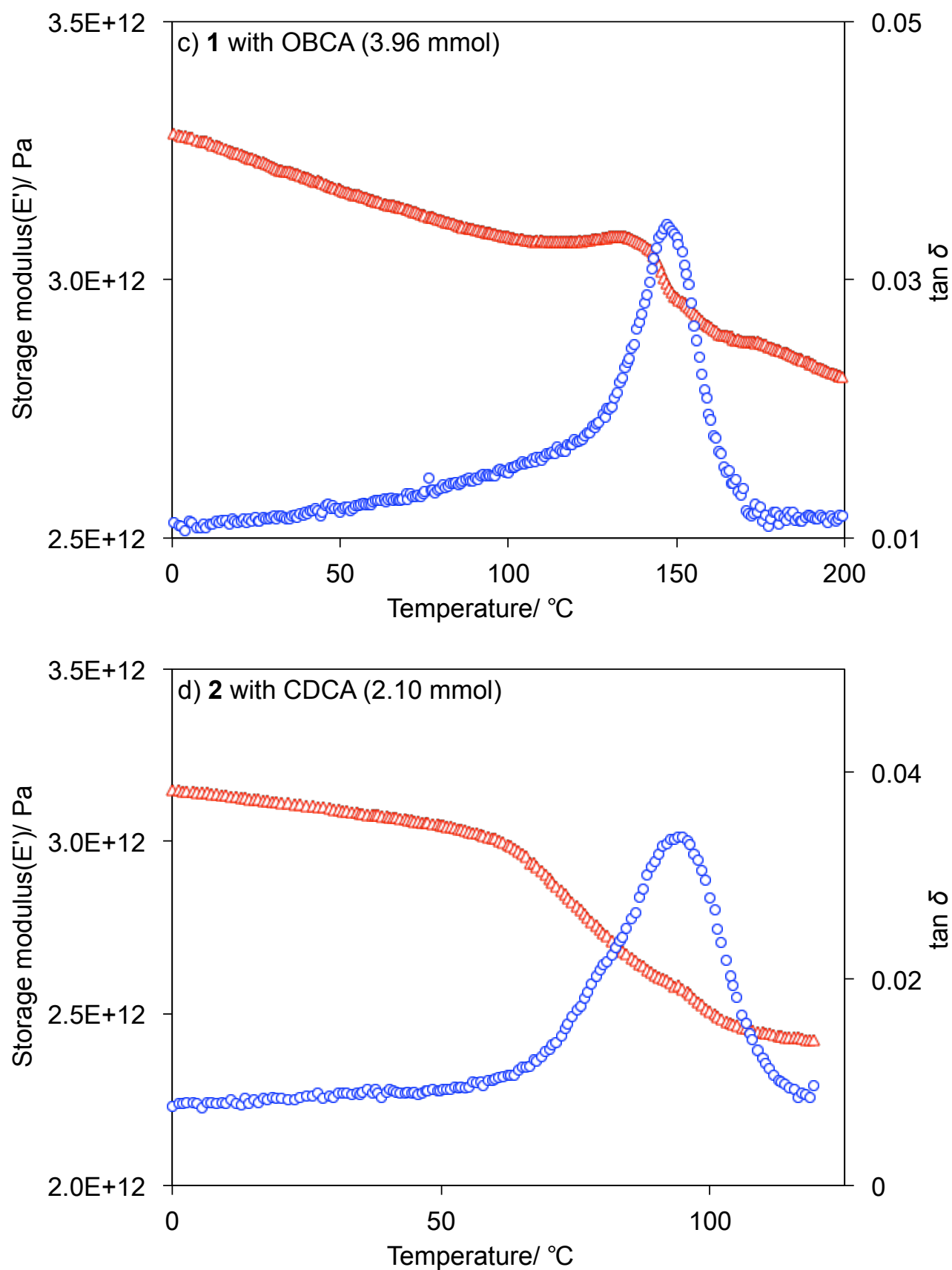


Fig. 8 Dynamic mechanical analysis thermograms of **1** with OBCA, a) 0.94 mmol, b) 2.10 mmol, c) 3.96 mmol, and d) **2** with 2.10 mmol CDCA hardened at 130 °C for 4 h. The storage modulus E' and $\tan \delta$ are represented by red open triangles and blue open circles, respectively.

Table 1 Bio-based carbon content, thermal stability, and thermal and mechanical properties of **1** and **2**.^a

Epoxy resin	Amount of hardener/mmol	Hardening time/h	Bio-based carbon content	T _{d5%} /°C ^b	T _g /°C ^c	Young's modulus/GPa ^d	Tensile strength/MPa ^d	Strain at breaking point/% ^d
1	2.10	1	38	317	115	0.9 ± 0.4	55.8 ± 5.3	6.1 ± 1.6
	2.10	2	38	293	116	1.3 ± 0.5	65.2 ± 4.3	6.0 ± 1.2
	2.10	3	38	328	116	1.2 ± 0.1	59.8 ± 5.0	5.3 ± 1.0
	0.94	4	21	292	28	0.37 ± 0.1	9.5 ± 1.3	69.3 ± 7.3
	2.10	4	38	310	115	1.6 ± 0.5	68.0 ± 11	5.2 ± 1.0
	3.94	4	53	287	146	2.8 ± 0.3	63.9 ± 25	3.9 ± 1.3
2	2.10	1	0	322	83	1.2 ± 0.1	66.7 ± 5.3	6.3 ± 1.8
	2.10	2	0	307	89	1.2 ± 0.3	67.8 ± 8.6	5.7 ± 1.2
	2.10	3	0	315	94	1.0 ± 0.2	63.0 ± 4.5	6.2 ± 1.1
	2.10	4	0	286	93	0.8 ± 0.2	68.0 ± 3.4	7.5 ± 1.8

^aHardened at 130°C and 5 MPa. ^bMeasured by thermal gravimetric analysis. ^cMeasured by dynamical mechanical analysis. ^dMeasured by tensile strength testing.